Effects of Laser Direct Intensity Modulation Index on Optical Beat Interference in Subcarrier Multiplexed Wavelength Division Multiple Access Networks

Mohammad M. Banat and Mohsen Kavehrad, *Fellow, IEEE*

Abstract- Degradation in carrier-to-interference ratio (CIR) due to optical beat interference (OBI) in subcarrier multiplexed wavelength division multiple Access (SCM/WDMA) networks using direct photodetection is evaluated. The subcarriers are assumed to directly intensity modulate separate lasers. A large signal model for the modulated laser light is used. The discrepancy in CIR between this model and the small signal model commonly used in the literature is important at high modulation indices (4.5 dB at about unity modulation index). This justifies the introduction of the large signal model for analyzing OBI. It is found from analytical results that OBI is lower for higher intensity modulation indices.

I. Introduction

Data transmission over optical fiber is capable of supporting very high bit rates. Various multiple access schemes have been studied in the past in an attempt to increase the achievable transmission capacity. Each of these schemes has its own merits and drawbacks. However, they all share a major disadvantage, that is, complexity. A multiple access scheme that offers highly reduced complexity as compared to other schemes was suggested in [1]. It uses wavelength division multiple access and subcarrier multiplexing as shown in Fig. 1.

Subcarrier multiplexing wavelength division multiple access (SCM/WDMA) provides a simple approach to maximizing the attainable transmission capacity. It is based on dividing the optical bandwidth into a number of optical channels each with a unique center frequency. Each optical carrier is intensity modulated by a set of RF subcarriers. Fig. 1 shows a schematic diagram of the hierarchy of the two multiplexing levels. There are N optical channels each with M RF subcarriers modulating it.

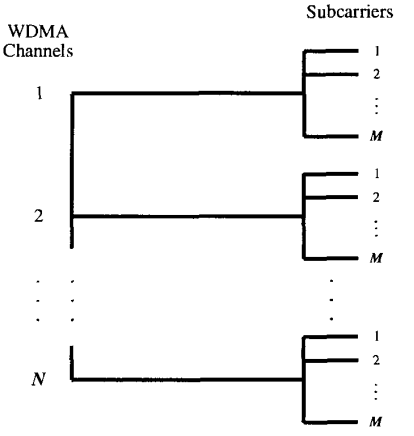

Fig. 1. Hierarchy of SCM/WDMA multiplexing schemes

Combined with direct detection, SCM/WDMA does not require complex circuitry for frequency stabilization. It does not require polarization control nor use of sharp optical filters. New users can be accommodated by the network without modifying the existing architecture, by simply adding more optical channels (see Fig. 1). Users can, as well, be added to any optical channel by introducing more subcarriers. SCM/WDMA does not require time synchronization between the transmitters and receivers. A block diagram of an SCM/WDMA network is shown in Fig. 2. With N wavelengths, the system supports communications links among MN users, as opposed to only N links in the case of conventional WDMA or FDMA.

The problem addressed in this paper is called optical beat interference (OBI) [2]. It is caused by the square envelope detection law of the photodetector (PD). To see that, consider the function of the PD in one of the user receivers. A total of M optical fields is present at the PD input. At the output of the PD, we would expect M terms representing the field intensities, plus $M(M-1)$ cross terms. If the spectral content of any one of these cross terms falls within the passband of the bandpass filter (BPF) in the intended user channel, it will cause interference. As will be shown, OBI can represent a serious limitation on the transmission capacity. In this paper, we present extensive analyses of the effect of increasing the laser intensity modulation index on OBI. The idea of

Paper approved by Matthew S. Goodman, the Editor for Optical Switching of the IEEE Communications Society. Manuscript received: December 16, 1993; revised September 15, 1994. This research was partially supported by the Telecommunications Research Institute of Ontario, Photonics Networks and Systems Thrust, and by the Jordan University of Science and Technology. This work includes portions of a Ph.D. dissertation by M. M. Banat, submitted to School of Graduate Studies and Research at the University of Ottawa in January 1995.

M. M. Banat is with the Department of Electrical Engineering, University of Ottawa, Ottawa, Ontario, Canada. He is leaving to the Jordan University of Science and Technology, Irbid, Jordan.

M. Kavehrad is with the Department of Electrical Engineering, University of Ottawa, Ottawa, Ontario, Canada.

IEEE Log Number 9411629.

increasing the modulation index to reduce OBI was introduced in [3] and [4].

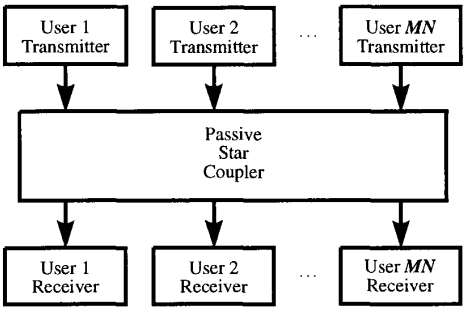

Fig. 2. SCM/WDMA system block diagram

This paper is organized as follows: In section II, we use for the first time, a large signal model to calculate the intensity modulated laser field spectrum. The results in section II are used in section III to evaluate the PD output CIR. Cases of zero and nonzero laser linewidths are considered. Main results appear in section IV. In section V, we present our main conclusions.

II. Large-Signal Laser Field Spectrum

Laser field spectra are needed for the calculation of the total field spectrum at the input of the PD. The input field spectrum is used to derive expressions for the PD output current spectrum, which is used in calculating the CIR at the input of the electronic processing circuitry. All fields are assumed to have the same polarization, a worst case assumption in the analyses of OBI [2]. Hence, spatial dependence of the fields is dropped in all derivations to follow. Let the electric field for the i-th user light signal be

$$e_i(t) = \left[S_i(t)\right]^{1/2} \cos\left[\varphi_i(t)\right] \tag{1}$$

where the intensity modulation is

$$S_i(t) = S_0\left\{1 + m\cos\left(\omega_i t\right)\right\} \tag{2}$$

The additional phase of the laser electric field can be decomposed into two components: a chirp component $\varphi_{mi}(t)$ and a phase noise component $\varphi_{ni}(t)$ modeled by a Wiener-Levy process. This assumption results in the familiar Lorentzian laser lineshape. The total phase is thus,

$$\varphi_i(t) = 2\pi F_i t + \varphi_{mi}(t) + \varphi_{ni}(t) \tag{3}$$

According to rate equations [5]

$$\begin{aligned}\dot{\varphi}_{mi}(t) &= \frac{\alpha}{2}\left[\frac{\mathrm{d}}{\mathrm{dt}}\left\{\ln S_i(t)\right\} + \frac{\kappa_s}{\tau_{ph}} S_i(t) - \frac{K_{tot} n_{sp}}{\tau_{ph}} \frac{1}{S_i(t)}\right] \\ &= \dot{\varphi}_{mi,1}(t) + \dot{\varphi}_{mi,2}(t) + \dot{\varphi}_{mi,3}(t)\end{aligned} \tag{4}$$

where $\varphi_{mi}(t)$ denotes the instantaneous laser frequency shift - due to chirp - from the operating frequency F_i. The various quantities in (4) are defined in Table-1. Substituting (2) in (4), and absorbing constant quantities in F_i we get

$$\dot{\varphi}_{mi}(t) = \sum_{n=1}^{\infty}\left[A_n \cos\left(n\omega_i t\right) + B_n \sin\left(n\omega_i t\right)\right] \tag{5}$$

where

$$A_n = \begin{cases} \dfrac{\alpha\kappa_s S_0 m}{2\tau_{ph}} + \dfrac{\alpha K_{tot} n_{sp}}{\tau_{ph} S_0 \sqrt{1-m^2}}\left[\dfrac{1-\sqrt{1-m^2}}{m}\right], & n = 1 \\ (-1)^{n+1} \dfrac{\alpha K_{tot} n_{sp}}{\tau_{ph} S_0 \sqrt{1-m^2}}\left[\dfrac{1-\sqrt{1-m^2}}{m}\right]^n, & n > 1 \end{cases} \tag{6}$$

$$B_n = (-1)^n \alpha\omega_i \left[\frac{1-\sqrt{1-m^2}}{m}\right]^n \tag{7}$$

The laser phase modulation due to chirp is thus,

$$\varphi_{mi}(t) = \sum_{n=1}^{\infty} \beta_n \cos\left(n\omega_i t + \psi_n\right) \tag{8}$$

where

$$\beta_n = (-1)^{n+1}\left[\left(-B_n/n\omega_i\right)^2 + \left(A_n/n\omega_i\right)^2\right]^{1/2} \tag{9}$$

$$\psi_n = -\tan^{-1}\left(\frac{A_n}{B_n}\right) \tag{10}$$

To find the number of significant terms in (8), one needs to look at typical values of various system parameters affecting the series. Values for such parameters are listed in Table-1. The value of κ_s is found from [6]

$$\kappa_s = \frac{\kappa}{2}\left(h\frac{c}{\lambda}\right)\frac{c}{\bar{n}}\alpha_m \tag{11}$$

where c is the speed of light in free space, h is Plank's

constant, and the other parameters are as in Table-1. S_0 is found from [5]

$$\kappa_s S_0 = \kappa P \tag{12}$$

TABLE 1: TYPICAL PARAMETER VALUES

Parameter	Symbol	Value	[Source], page
Subcarrier frequency	f_i	5.0 GHz	
Operating wavelength	λ	1.55 μm	
Linewidth enhancement factor	α	5.0	[6], 227
Output power per laser facet	P	3.0 mW	[5], 121
Effective refractive index	$\bar{n}$	3.5	[5], 27
Nonlinear power gain coefficient	κ	4.4/W	[5], 121
Mirror loss	α_m	4500/m	[6], 227
Total spontaneous emission enhancement factor	K_{tot}	1.0	[5], 44
Spontaneous emission coefficient	n_{sp}	1.7	[5], 15
Photon lifetime	τ_{ph}	1.0 ps	[5], 121
Nonlinear photon number gain coefficient	κ_s	1.008×10^{7}	
Unmodulated (average) photon number	S_0	1.2×10^{5}	

From (6), (7), (9), and (10), values for the first few coefficients in (8) are computed as in Table-2. In these calculations, the modulation index is assumed to be 0.9. Fewer terms in (8) are needed at smaller modulation indices. Based on the data in Table-2, A_n and ψ_n will be neglected and only the first three terms of β_n will be kept. Thus,

$$\varphi_{mi}(t) = \sum_{n=1}^{3} \beta_n \cos(n\omega_i t) \tag{13}$$

where

$$\beta_n = -\frac{B_n}{n\omega_i} = \frac{(-1)^{n+1}}{n}\alpha\left[\frac{1-\sqrt{1-m^2}}{m}\right]^n \tag{14}$$

For very small $m \le 0.3$, β_1 is the only significant coefficient, and the approximation

$$\sqrt{1-m^2} \approx 1-\frac{m^2}{2} \tag{15}$$

can be used to find the small-signal frequency modulation index

$$\beta \approx \frac{\alpha m}{2} \tag{16}$$

This is the widely used expression for the frequency modulation index [4]. As shown above, it is a good enough approximation only if $m \le 0.3$ while otherwise (14) should be used. Substituting (3) into (1) gives the i-th user field as:

$$e_i(t) = \left[S_i(t)\right]^{1/2} \cos\left[2\pi F_i t + \varphi_{ni}(t) + \varphi_{mi}(t)\right] \tag{17}$$

TABLE 2: FIRST FEW COEFFICIENT VALUES IN (8)

n	$B_n/n\omega_i$	$A_n/n\omega_i$	β_n	ψ_n
1	-4.074	1.219	4.252	0.29
2	1.277	-1.32×10^{-3}	-1.277	0
3	-0.534	5.517×10^{-4}	0.534	0
4	0.251	-2.594×10^{-4}	-0.251	0
5	-0.126	1.301×10^{-4}	0.126	0

The equivalent complex representation of (17) is

$$\begin{aligned}\tilde{e}_i(t) &= \left[S_i(t)\right]^{1/2} e^{j\varphi_{mi}(t)} e^{j\varphi_{ni}(t)} e^{j2\pi F_i t} \\ &= e_{il}(t)\tilde{e}_{mi}(t)\tilde{e}_{ni}(t)e^{j2\pi F_i t} \\ &= E_i(t)e^{j2\pi F_i t}\end{aligned} \tag{18}$$

The corresponding power spectral densities (PSD's) are known to be related by

$$S_{e_i}(f) = \frac{1}{4}\left[S_{\tilde{e}_i}(f) + S_{\tilde{e}_i}(-f)\right] \tag{19}$$

$$S_{\tilde{e}_i}(f) = S_{E_i}(f - F_i) \tag{20}$$

$$S_{E_i}(f) = S_{e_{il}}(f) * S_{\tilde{e}_{mi}}(f) * S_{\tilde{e}_{ni}}(f) \tag{21}$$

Because $f_i << F_i$, the term $S_{e_{il}}(f)$ that represents the PSD contribution of $\left[S_i(t)\right]^{1/2}$ will be assumed equal to a constant S_0. The phase noise spectrum can be shown to be given by [5]

$$S_{\tilde{e}_{ni}}(f) = \frac{2}{\pi\Delta f\left(1+\frac{2f}{\Delta f}\right)^2} = \Phi(f) \tag{22}$$

Next we calculate the chirp contribution to the PSD, $S_{\tilde{e}_{mi}}(f)$. From (18)

$$\tilde{e}_{mi}(t) = e^{j\varphi_{mi}(t)} = \exp\left[j\sum_{n=1}^{3}\beta_n\cos(n\omega_i t)\right] \tag{23}$$

which can be expanded in the following series

$$\begin{aligned}\tilde{e}_{mi}(t) = &\sum_{k_1=-\infty}^{\infty}\sum_{k_2=-\infty}^{\infty}\sum_{k_3=-\infty}^{\infty} J_{k_1}(\beta_1)J_{k_2}(\beta_2)J_{k_3}(\beta_3) \\ &\times\exp\left[j\sum_{l=1}^{3}k_l\left(l\omega_i+\frac{\pi}{2}\right)\right]\end{aligned} \tag{24}$$

where $J_r(x)$ is a Bessel function of the first kind of order r. Changing summation indices yields

$$\begin{aligned}\tilde{e}_{mi}(t) = &\sum_{n=-\infty}^{\infty}\sum_{k_2=-\infty}^{\infty}\sum_{k_3=-\infty}^{\infty} J_{n-2k_2-3k_3}(\beta_1)J_{k_2}(\beta_2)J_{k_3}(\beta_3) \\ &\times\exp\left[j\left\{n\omega_i t+(n-k_2-2k_3)\frac{\pi}{2}\right\}\right]\end{aligned} \tag{25}$$

Note that, (25) shows the coefficients of the individual harmonics of f_i. Note, furthermore, that the phases of the different terms involving f_i are not the same. Hence, the effects of these terms in the power spectrum add noncoherently. As a result, the chirp spectrum is

$$\begin{aligned}S_{\tilde{e}_{mi}}(f) = &\sum_{n=-\infty}^{\infty}\delta(f-nf_i) \\ &\times\left[\sum_{k_2=-\infty}^{\infty}\sum_{k_3=-\infty}^{\infty} J^2_{n-2k_2-3k_3}(\beta_1)J^2_{k_2}(\beta_2)J^2_{k_3}(\beta_3)\right]\end{aligned} \tag{26}$$

Since $S_{e_{il}}(f)$ is assumed constant; the PSD of the complex field becomes

$$S_{\tilde{e}_i}(f) = S_0\sum_{n=-\infty}^{\infty}A^2(n)\Phi(f-F_i-nf_i) \tag{27}$$

where

$$A^2(n) = \sum_{k_2=-\infty}^{\infty}\sum_{k_3=-\infty}^{\infty} J^2_{n-2k_2-3k_3}(\beta_1)J^2_{k_2}(\beta_2)J^2_{k_3}(\beta_3) \tag{28}$$

The spectrum of the real field is thus,

$$\begin{aligned}S_{e_i}(f) = &\frac{S_0}{4}\sum_{n=-\infty}^{\infty}A^2(n) \\ &\times\Phi(f-F_i-nf_i)+\Phi(f+F_i+nf_i)\end{aligned} \tag{29}$$

III. Photodetector Output CIR

The front end of the receiver is an optical filter centered on the optical frequency of the intended user channel (Fig. 3). Out of MN fields incoming to the filter, only M continue their way to the PD. The center frequency of the optical filter is denoted by F_0.

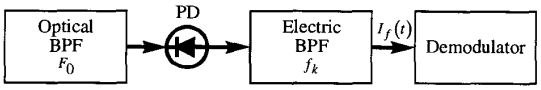

Fig. 3. Intended user receiver

All M users in the same optical channel have identical optical filters. The total field $e(t)$ at the input of the PD is

$$e(t)=\sum_{i=1}^{M} e_i(t) \tag{30}$$

The PD converts this field into an electric signal proportional to the field intensity. Since we are calculating signal-to-interference ratios, the constant of proportionality will be set to unity. This yields the PD output as

$$I(t)=|e(t)|^2=\mathrm{LP}\left\{\sum_{i=1}^{M}\sum_{l=1}^{M} e_i(t)e_l(t)\right\} \tag{31}$$

where LP denotes taking the low pass part. The right hand side of (31) can be broken into a signal component $I_s(t)$ and a cross term component $I_c(t)$ as follows

$$\begin{aligned} I(t)&=\mathrm{LP}\left\{\sum_{i=1}^{M} e_i(t)+2\sum_{i=1}^{M-1}\sum_{l=i+1}^{M} e_i(t)e_l(t)\right\} \\ &=I_s(t)+I_c(t) \end{aligned} \tag{32}$$

The PSD of a two-term sum of the form in (31) is given in [7]. This result can be generalized for the M-field sum in (31) in the form

$$\begin{aligned} S_I(f)&=|H_{det}(f)|^2 \\ &\quad\times\left[\sum_{i=1}^{M} S_{I_i}(f)+4\sum_{i=1}^{M-1}\sum_{l=i+1}^{M} S_{e_i}(f)*S_{e_l}(f)\right] \\ &=S_{I_s}(f)+S_{I_c}(f) \end{aligned} \tag{33}$$

The first two terms in (33) correspond to the first two terms in (32), respectively. The effect of the low pass operator in the time domain is equivalent to multiplication by $|H_{det}(f)|^2$ in the frequency domain. For the sake of simplicity, $|H_{det}(f)|^2$ will be set to unity in the subcarrier frequencies range and to zero, otherwise.

To calculate the ratio of the signal power to the interference power, we need to evaluate both powers at the output of the BPF. Assuming user number k, transmitting at f_k, is the intended one, the BPF must have its frequency response maximum around f_k

$$|H_k(f)|=\begin{cases}1, & f_k-B/2<f<f_k+B/2\\ 0, & \text{Otherwise}\end{cases} \tag{34}$$

To determine the signal power, we need to evaluate $I_s(t)$ in (32) by using (1) and (2)

$$I_s(t)=\frac{S_0}{2}\sum_{i=1}^{M}\left[1+m\cos(\omega_i t)\right] \tag{35}$$

At the output of the BPF, only the intended user signal appears. Hence, the filtered signal PSD is

$$S_{I_{sf}}(f)=\frac{S_0^2m^2}{16}\left[\delta(f-f_k)+(f+f_k)\right] \tag{36}$$

The total signal power is thus,

$$P_s=\frac{S_0^2m^2}{8} \tag{37}$$

In the following two subsections, we find the beat noise power for lasers with zero linewidths and lasers with nonzero linewidths.

A. Lasers with a Zero Linewidth

This is a worst case assumption as far as OBI is concerned; because all the power in an interference term centered on f_k will pass through the electric BPF in the receiver. The phase noise contribution to the field spectrum in (29) is assumed to be

$$\Phi(f)=\delta(f) \tag{38}$$

Hence, repeating for $I_c(t)$ what has been done above for $I_s(t)$, one obtains

$$I_c(t)=\mathrm{LP}\left\{2\sum_{i=1}^{M-1}\sum_{l=i+1}^{M} e_i(t)e_l(t)\right\} \tag{39}$$

Thus, the beat noise PSD is

$$S_{I_c}(f) = \mathrm{LP}\left\{4\sum_{i=1}^{M-1}\sum_{l=i+1}^{M} S_{e_i}(f) * S_{e_l}(f)\right\}$$
$$= \frac{S_0^2}{4}\sum_{i=1}^{M-1}\sum_{l=i+1}^{M}\sum_{n=-\infty}^{\infty}\sum_{r=-\infty}^{\infty} A^2(n)A^2(r) \quad (40)$$
$$\times\left\{\delta(f - nf_i + rf_l) + \delta(f + nf_i - rf_l)\right\}$$

This is the beat noise PSD at the input of the BPF. The beat noise power at the filter output is

$$P_{obi} = 2\int_{f_k - B/2}^{f_k + B/2} S_{I_c}(f)\,df \quad (41)$$

To calculate the last integral, one has to find out which frequency components in (40) are in the passband of $H_k(f)$. To do so, we'll let the subcarrier frequencies be integer multiples of the filter bandwidth B away from a frequency offset f_0, i.e.,

$$f_i = f_0 + iB \quad (42)$$

A typical frequency component in (40) is

$$nf_i - rf_l = (n - r)f_0 + (ni - rl)B \quad (43)$$

For this component to interfere with the intended user signal, the following condition on n and r must be satisfied

$$(n - r)f_0 + (ni - rl)B = f_k = f_0 + kB \quad (44)$$

which can be transformed into

$$(n - r - 1)f_0 + (ni - rl - k)B = 0 \quad (45)$$

As a result, we can write the interference power in (41) in the form

$$P_{obi} = \frac{S_0^2}{2}\sum_{i=1}^{M-1}\sum_{l=i+1}^{M}\left[\sum_{n=-\infty}^{\infty}\sum_{r=-\infty}^{\infty} A^2(n)A^2(r)\right]_{n,r\ \text{satisfy (45)}} \quad (46)$$

Finally, the carrier-to-interference ratio obtained by dividing (37) by (46) is

$$CIR = \frac{m^2}{4\sum_{i=1}^{M-1}\sum_{l=i+1}^{M}\left[\sum_{n=-\infty}^{\infty}\sum_{r=-\infty}^{\infty} A^2(n)A^2(r)\right]_{n,r\ \text{satisfy (45)}}} \quad (47)$$

B. Lasers with Nonzero Linewidths

An actual laser never has a zero linewidth. Hence, the phase noise contribution in (29) will be substituted for from (22). Similar to the previous subsection, the beat noise PSD can be written as

$$S_{I_c}(f) = \frac{S_0^2}{4}\sum_{i=1}^{M-1}\sum_{l=i+1}^{M}\sum_{n=-\infty}^{\infty}\sum_{r=-\infty}^{\infty} A^2(n)A^2(r)$$
$$\times\left\{\Phi^{(2)}(f - nf_i + rf_l) + \Phi^{(2)}(f + nf_i - rf_l)\right\} \quad (48)$$

where

$$\Phi^{(2)}(f) = \Phi(f) * \Phi(f) = \frac{1}{\pi\Delta f}\frac{1}{1 + (f/\Delta f)^2} \quad (49)$$

Substituting (48) and (49) into (41) and integrating yields

$$P_{obi} = \frac{S_0^2}{2}\sum_{i=1}^{M-1}\sum_{l=i+1}^{M}\sum_{n=-\infty}^{\infty}\sum_{r=-\infty}^{\infty} A^2(n)A^2(r)Q(k, ni, rl) \quad (50)$$

where

$$Q(k, ni, rl) = \frac{1}{\pi}\tan^{-1}\left\{\frac{B}{\Delta f}\left(k + \frac{1}{2} - ni + rl\right)\right\} - \frac{1}{\pi}\tan^{-1}\left\{\frac{B}{\Delta f}\left(k - \frac{1}{2} - ni + rl\right)\right\} \quad (51)$$

Dividing (37) by (50) provides the signal-to-interference ratio in the k-th user channel as

$$CIR = \frac{m^2}{4\sum_{i=1}^{M-1}\sum_{l=i+1}^{M}\left[\sum_{n=-\infty}^{\infty}\sum_{r=-\infty}^{\infty} A^2(n)A^2(r)Q(k, ni, rl)\right]} \quad (52)$$

IV. Results

CIR values in (47) and (52) are computed for the case when the number of subcarriers per optical carrier is 20, i.e., $M = 20$. Subcarrier frequencies assumed values of 1, 2, ..., 20 GHz. The electric BPF bandwidth is 1 GHz. From these numbers, the initial frequency offset is $f_0 = 0$. In the zero laser linewidth case, they also simplify the condition in (45) such that we compute terms in (46) and (47) that satisfy

$$r = \left[\frac{ni-k}{l}\right]_{r \text{ is integer}} \tag{53}$$

Fig. 4 shows a plot of the carrier-to-interference ratio in channel number 10 as a function of the intensity modulation index in the zero laser linewidth case. The curve for (47) is denoted 'the large-signal approximation'. Shown also on the same graph is the small-signal approximation to CIR as obtained in [4]. The same curve could also be obtained by keeping only one term instead of three in (13), and using the small-signal approximation to the frequency modulation index in (16). From Fig. 4 two observations are obvious. First, CIR is higher for larger intensity modulation indices. Second, there is about 4.5 dB difference between the small- and the large-signal models in the calculated CIR value at larger modulation indices close to unity.

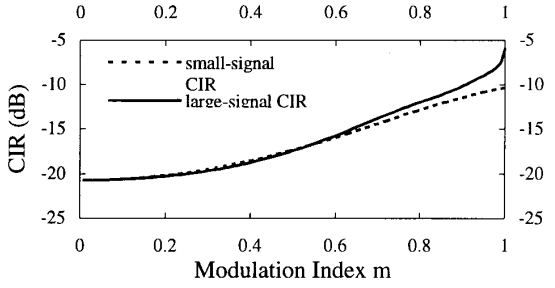

Fig. 4. Small- and large-signal CIR approximations

The first observation stems from the fact that a higher intensity modulation index implies a wider spread of the modulated laser field spectrum. When two laser fields are mixed at the PD, the resulting field bandwidth is roughly the sum of the bands of the two fields. When the individual fields' spectra are wider, the fraction of interference terms that falls within the passband of the electric BPF is naturally less. Hence, the improvement in CIR is expected.

The second observation can be explained as follows. Small signal model neglects many terms in the modulated laser field phase. These terms amount to a further field spread, reducing OBI and improving CIR. The discrepancy between the two models is high at modulation indices approaching unity. This difference can result in misleading conclusions about the severity of OBI.

Fig. 5 illustrates the effect of OBI on different subcarrier channels for a modulation indices of 0.5. Laser linewidths were set to zero.

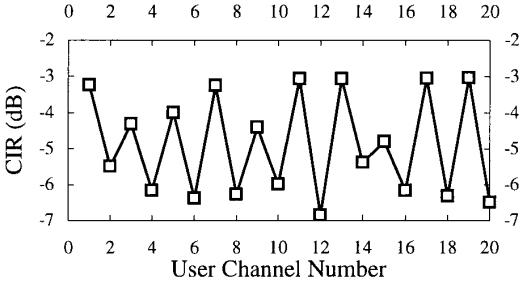

Fig. 5. OBI in user channels for $m = 1.0$

The main observation in Fig. 5 is that the CIR has local maxima for odd-numbered channels. This is to be expected because, according to the subcarrier frequency assignment we are adopting, the subcarrier channel number equals the subcarrier frequency in GHz (e.g., subcarrier frequency of user 8 is 8 GHz). For odd-numbered channels, it is less frequent than it is for other channels to find terms in (47) that satisfy (53). This motivates a suggestion for assigning subcarrier frequency values that are prime to each other. In fact, from Fig. 5, this can lead to an improvement of several dB's in the CIR. This can be done, for example, by choosing 3, 5, 7, 11, ... GHz as the subcarrier frequencies. In general, the subcarrier frequencies can be chosen to be prime multiples of the electric BPF bandwidth B.

Fig. 6 shows the effect of nonzero laser linewidth on the CIR as a function of the modulation index. As the figure demonstrates, there is very little effect of the laser linewidth on the CIR at high modulation indices. This is because, at such indices, optical fields are already spread over wide bands due to deep modulation. Laser linewidths add only a little more broadening to the field spectra.

V. Conclusions

An analytical model has been developed for analysis of large-signal laser modulation. This model has been used to evaluate the large-signal laser field spectrum. Furthermore, it has been used to analyze the effect of increasing the intensity modulation index on optical beat interference performance of SCM/WDMA networks. It has been confirmed through analysis and graphs that increasing the modulation index helps to reduce the SCM/WDMA network performance degradation due to OBI. Graphs of the CIR vs. the modulation index demonstrated the importance of introducing the large signal analysis model. Plotting the CIR vs. the user channel number revealed the fact that significant improvements in the CIR could be attained by careful assignment of the subcarrier frequencies such that they are prime to each other.

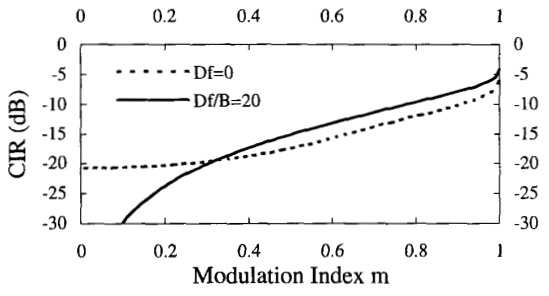

Fig. 6. Effect of laser linewidth on OBI

REFERENCES

[1] N. K. Shankaranarayanan, S. D. Elby, and K. Y. Lau, "WDMA/Subcarrier-FDMA Lightwave Networks: Limitations due to Optical Beat Interference,", *J. Lightwave Tech.*, Vol. 9, No. 7, pp. 931-943, Jul. 1991

[2] M. M. Banat and Mohsen Kavehrad, "Reduction of Optical Beat Interference in SCM/WDMA Networks using Pseudorandom Phase Modulation,", *J. Lightwave Tech.*, Vol. 12, No. 10, pp. 1863-1868, Oct. 1994

[3] T. H. Wood and N. K. Shankaranarayanan, "Measurements of the Effect of Optical Beat Interference (OBI) on the Bit-Error-Rate of a Subcarrier-Based Passive Optical Network (PON),", *OFC'93*, pp. 231-233

[4] T. H. Wood and N. K. Shankaranarayanan, "Operation of a Passive Optical Network with Subcarrier Multiplexing in the Presence of Optical Beat Interference,", *J. Lightwave Tech.*, Vol. 11, No. 10, pp. 1632-1640, Oct. 1993

[5] K. Petermann, *Laser Diode Modulation and Noise*, Kluwer Academic Publishers, Tokyo, 1988

[6] D. P. Agrawal and N. K. Dutta, *Long-Wavelength Semiconductor Lasers*, Van Nostrand Reinhold Company, New York, 1986

[7] M. Nazarthy, W. V. Sorin, D. M. Baney, and S. A. Newton, "Spectral Analysis of Optical Mixing Measurements,", *J. Lightwave Tech.*, Vol. 7, No. 7, pp. 1083-1096, Jul. 1989

Mohammad M. Banat was born in Irbid, Jordan in 1963. He received the B.Sc. and M.Sc. degrees, both in electrical engineering, from Yarmuk University, Jordan, in 1984 and 1986, respectively, and the Ph.D. degree in electrical engineering from the University of Ottawa in 1995. During the academic year of 1986/1987, he taught electrical engineering courses at the Hijjawi College of Technology, Yarmuk University, Jordan, and worked as a teaching assistant at the Department of Electrical Engineering, Jordan University of Science and Technology. Between 1987 and 1989 he served as a communications engineer at the Jordanian Civil Defense Communications Department. In 1989 he joined the Department of Electrical Engineering at the University of Petroleum and Minerals, Saudi Arabia, where he was engaged in research on echo cancellation on voice-band data transmission networks. In September 1991 he joined the University of Ottawa, Canada, to work towards the Ph.D. degree. In February 1995, he will be joining the Department of Electrical Engineering at the Jordan University of Science and Technology. His current research interests are in wavelength division multiplexing and subcarrier multiplexing lightwave networks.

Mohsen Kavehrad (SM'86-F'92) was born in Tehran, Iran, on January 1, 1951. He received his B.S. degree from Tehran Polytechnic Institute, Iran, in 1973, M.S. degree from Worcester Polytechnic Institute, Worcester, MASS., in 1975, and Ph.D. degree from Polytechnic Institute of New York (now: Polytechnic University), Brooklyn, NY., in Nov. 1977, all in Electrical Engineering. Between 1978 and 1981, he worked for Fairchild Industries (Space Communications Group), GTE Satellite Corp., and GTE Laboratories in Waltham-Mass. In December 1981 he joined AT&T Bell Laboratories where he worked in Research, Development, and Systems Engineering Areas as a member of technical staff. In March 1989 he joined the Department of Electrical Engineering at University of Ottawa, as a Full Professor. He is the Leader of Photonic Networks and Systems Thrust and a Project Leader in the Telecommunications Research Institute of Ontario (TRIO). Also, he is a project leader in the Canadian Institute for Telecommunications Research (CITR). Presently, he is the Director of Ottawa-Carleton Communications Center for Research (OCCCR), an entity shared by Carleton University and University of Ottawa. In summer of 1991, he was a visiting researcher at NTT Laboratories in Japan. He also worked on satellite communications, point-to-point microwave radio communications, portable and mobile radios communications, atmospheric laser communications and on optical fiber communications and networking. He has also worked on multiple access networks, routing and flow control problems in packet switched networks. He has published over 120 and has several patents issued or pending in these fields. He has been a technical consultant of BNR in Ottawa, NTT Labs in Japan and a number of other industries. He is a former Technical Editor for the IEEE Magazine of Lightwave Telecommunication Systems, IEEE Transactions on Communications and the IEEE Communications Magazine. He has organized and chaired sessions at a number of IEEE Communications Society international conferences and has been on conference program committee for the Optical Society of America.